ISSN: 2277-3754
ISO 9001:2008 Certified
International Journal of Engineering and Innovative Technology (IJEIT)
Volume 2, Issue 12, June 2013

Characterization of Bond Coats Produced by High Velocity Oxy-Fuel and Cold Gas Dynamic Sprayed N_2 Gas

W.S.Rathod, A.S.Khanna, R.C.Rathod
Corrosion Science & Engineering Dept, IIT, Bombay Mumbai, India
VNIT, Metallurgy Dept, Nagpur, India

Abstract-To protect hot- sections of power generation components of gas turbine and aircraft, thermal barrier coatings (TBC's) are widely used. Conventional TBC's consist of a MCrAlY alloys (where M stand for Co, Ni or FeNi etc,) bond coating for oxidation resistance and a ceramic top coating for thermal insulation (mainly yttria stabilized zirconia, YSZ). The purpose of the current study was to investigate the microstructure and oxidation behavior of CoNiCrAlY coatings, deposited by the HVOF and CGDS techniques. The quality of the as-sprayed and oxidized bond coats was assessed in terms of their microstructure, especially porosity and oxide inclusion and mechanical properties, especially hardness. Sprayed samples were exposed to isothermal oxidation at 900 ^{0}C in air. Oxide growth rates were obtained from a series of mass gain measurements, while oxide scale compositions were determined using SEM, XRD and EDX analysis. Results obtained in this study show HVOF coating features high levels of visible defects, oxide content, spinel- type oxide and high oxide growth rate, whereas CGDS coatings show low oxide growth rate as a result of low porosity, oxide content and high hardness. The oxide scale on the CGDS coating after 1000 hrs of oxidation was composed of alumina and initiation of spinal type of oxides.

***Index Terms*— Cold Gas Dynamic Spray (CGDS), High velocity oxygen-fuel (HVOF), bond coat.**

I. INTRODUCTION

Thermal barrier coatings (TBC) are used for gas turbine blades of power plants and aircraft engines for higher efficiency and long term durability. TBC system consists of MCrAlY bond coat and YSZ top coat. Bond coat enhances the adhesion of the ceramic top coat. Working conditions at elevated temperature lead to the oxidation of the bond coat which causes the formation of a thermally grown oxide (TGO) layer at the bond coat/ top coat interface and continues to grow in thickness during thermal cycling by consuming the oxidation resistant element reservoir [1]. Rapid and uneven growth of the TGO leads to localized stress concentrations where cracks can nucleate and initiate the failure dynamics [2, 3]. If TGO layer consists of a dense, continuous and adhesive alumina (α- A_2O_3) scale, it acts as a diffusion barrier and thus inhibits further oxidation due to its low diffusivity. Formation of additional oxides in TGO, Such as (NiO, CoO,Cr_2O_3) or mixed spinel- type oxide such as chromia/alumina ($(CrAl)_2O_3$), spinel ($(NiCrAl)_2O_4$) which have high growth rates, cause increase in TGO thickness and thus are detrimental as they form protrusion in the TGO that initiates failure mechanisms of the top coat. The oxidation resistance and the TGO quality depend, not only on the chemical composition but also on the technique used to produce the bond coat. CoNiCrAlY is typically coated by VPS (Vacuum plasma spraying), APS (Air-plasma spraying), LPPS (Low pressure plasma spraying) and HVOF (High velocity oxygen-fuel spraying) [4, 6]. The drawback of these techniques is that their inherent elevated temperature inevitably leads to changes in the coating microstructure namely oxide inclusions. APS gives a coating which has porosity and oxide impregnation. VPS represents the state of the art technology for the bond coat deposition, but the cost is relatively high due to vacuum operation. Shibata et al. [4] deposited CoNiCrAlY bond coat using APS, LPPS and HVOF and the extent of oxide contamination was 1.8, 0.16 and 0.94 wt. % respectively. F. Tang et al. [7] deposited CoNiCrAlY coating by HVOF and reported that in process surface oxidation is detrimental to the TGO growth mechanism as it promotes the onset undesirable fast- growing no alumina oxides that form protrusions and cause the TBC failure mechanisms. An alternative to above process is cold gas dynamic spray (CGDS) technique. In the CGDS spraying, the kinetic energy, rather than thermal energy is used to produce the bond coat [8-12]. In this process, the fine powders particles (5-42 μm dia) are propelled in a supersonic flow and get deposited on substrate after undergoing sever plastic deformation upon impacting the substrate**.** CGDS coating operates at lower temperatures and also uses inert gases such as helium and nitrogen which hinder oxidation and grain growth during deposition [13, 15]. Resent researches have showed the potential of CGDS compared to other VPS [23]. P. Richer et al. [16, 17] deposited CoNiCrAlY coating using CGDS sprayed with He gas reported that coating composed of alumina, without the presence of NiO or spinal-type mixed oxides. Q. Zhang et al. [18] studied oxidation behavior of NiCrAlY coatings deposited using CGDS technique. They reported the formation of (α-A_2O_3) at 900^{0}C and 1000^{0}C. The aim of the present work, therefore, is to compare the oxidation behavior of the bond coat material (CoNiCrAlY), applied using both techniques. The difference in the coating characteristics is expected due to the large difference in kinetic energy of deposition which in turn can modify the oxidation behavior of the coatings.

ISSN: 2277-3754
ISO 9001:2008 Certified
International Journal of Engineering and Innovative Technology (IJEIT)
Volume 2, Issue 12, June 2013

II. EXPERIMENTAL WORK

A. Feedstock powder

The feedstock material chosen in this study is a commercially available CoNiCrAlY alloy, purchased from M/s. Metallizing Equipment Pvt. Ltd. Jodhpur, trade name MEC 9950 AMF powder with a nominal composition of CoNiCrAlY. The detail of the powder used to carry out the work is shown in Table1.

Table. 1 Chemical Composition of Powder

Elements →	Co	Ni	Cr	Al	O	Y
Wt % →	38.25	32.33	20.51	8.90	0	0.01

Fig.1 illustrates the cumulative result obtained from particle size analyzer (Laser Diffraction LS 13320) for powder. The distribution of particles size is homogenous with an average of approximately 32µm.

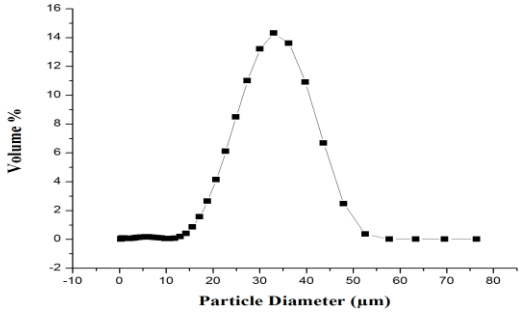

Fig.1 Plot of Cumulative Volume % Particle Diameter For The As-Received Conicraly Powder

B. CoNiCrAlY powder characterization

Fig.2 shows XRD results of CoNiCrAlY powder, surface morphology and EDX analysis of elemental composition (wt. %) at selected points. This gas atomized powder has a spherical morphology and particle size range (10-42 µm dia.). The observed composition of the powder is in considerable agreement to that supplied by the supplier, except for a small concentration of yttrium. Since the γ phase is a solid solution of Co, Ni, Cr etc. and has a higher mean atomic number, it appears brighter in BSE mode. Hence, the brighter phase is represented by γ and the darker phase as β-NiAl/CoAl, which has a lower mean atomic number and hence lower contrast in BSE mode, as confirmed in references [16-20].

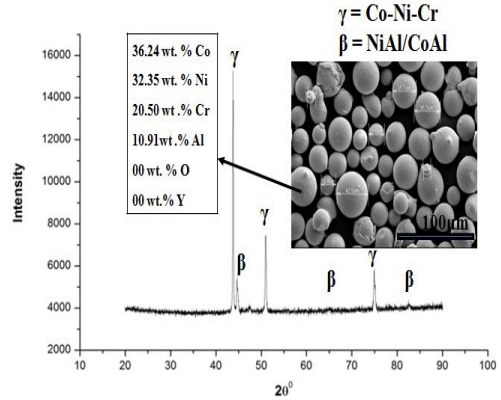

Fig. 2 XRD Pattern of Conicraly Powder Revealing A Two-Phases, Γ+B Structure

C. Deposition techniques and equipment

Cold spray is a relatively low temperature process with deposition carried out in the solid state. In cold spray process, the penning effect of incoming high velocity solid particles deforms the deposited material which tends to close any small pores or gaps in the underlying material [9, 11, 15 and 17]. In order to understand the effect of N_2 carrier gas was employed to carry and accelerate the CoNiCrAlY powder. The 316L stainless steel plates were cut into 300x300x2 mm size with a wheel cutter. Before the deposition, the plates were grit blasted with 20- grit alumina at a pressure of 0.3 MPa to increase surface roughness and ultrasonically cleaned in water and ethanol. Then cold spray process was carried out at M/s ASB, Industries, Inc Barberton at Ohio, USA. Finally plates were cut into small pieces of (10x10x2mm) size using wire electrical discharge machine for experiment. HVOF coating was carried out using HIPOJET-2700 model, courtesy M/s Metallizing Equipment Co.Pvt. Ltd., Jodhpur at their premises at Jodhpur, using nitrogen as carrier gas. Hardness values of as-sprayed the CGDS and HVOF coatings were measured with one of the latest methods of assessing the hardness of the thin coated layer by nanoindentation. The as-sprayed sample was mounted in epoxy resin and subsequently polished. Hardness measurement was carried out on as-sprayed sample on cross-section of the coating using Triboindeneter (Hysitron). The indentations were performed perpendicularly to the substrate interface; the distance between the indentations was kept equal to 30Nm, to avoid a mutual influence of consecutive responses. The load 11000 grams applied for 15 s. Six (6) indents are made on each sample and averages of the results were taken. The as-sprayed sample was mounted in epoxy resin and subsequently polished. Surface morphologies of as-deposited and oxidized samples were investigated to assess the properties in the as-sprayed and oxidized samples using SEM. The coated samples were sectioned and polished using standard metallographic techniques to observe the coating cross-section.

III. RESULTS & DISCUSSION

A. Characterization of as sprayed Coatings

1 As-sprayed HVOF coating

Fig. 3 (a, b, c) show the surface morphology, cross-sectional morphology and dendrites microstructure of as- sprayed HVOF coating. The microstructure of coating revealed semi-melted particles presented on the top of as-sprayed condition. The coating surface is rough in the as-sprayed condition due to the presence of melted and unmelted particles. The thicknesses of the coatings measured, is in the range 165-299µm. Coating shows, the dendrites are well packed and well interlocked to each other as shown in Fig. 4(b).

ISSN: 2277-3754
ISO 9001:2008 Certified
International Journal of Engineering and Innovative Technology (IJEIT)
Volume 2, Issue 12, June 2013

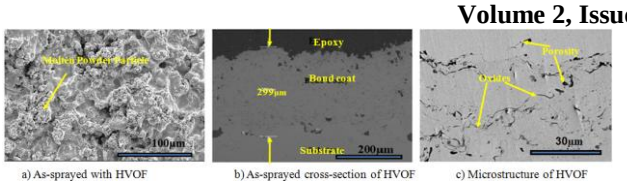

Fig. 3 SEM images of HVOF coating in as-sprayed condition

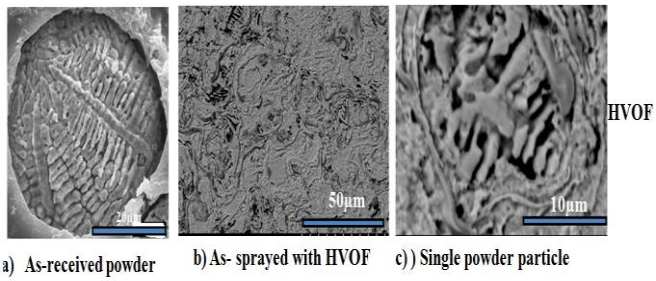

Fig. 4 (a) Secondary electron SEM images of etched cross section of powder revealing dendritic structure (b) As-sprayed HVOF cross-section revealing deformed dendrites (c) Single Powder particle revealing rapid solidification of small globules flattened from striking a cold surface at high velocities

The microstructure of the coating is less dense due to more porous as compared to CGDS. Fig. 4 (c) shows the sub layer of HVOF indicating melting of the particles and thus resulting in shrinkage of dendrites and thus results in rapid solidification of small globules. Most of the dendrites appear to be deformed significantly giving a flattened appearance as compared to original dendrites of the feedstock powder (Fig.4 (a)). The EDAX analysis was carried out on surface. Coating was almost same as the composition of the sprayed powder with small amount of O.

2. CGDS with N_2 gas

Figure.5 (a) shows individual powder particles, not properly adhered to the surface, perhaps due to not acquiring the critical velocity required for the deposition. Hence, multi-impacts under N_2 carrier gas display relatively higher degree of porosity, portraying low carrying capability of accelerating gas (Fig.5 (b)). This behavior is due to the increase in density of the carrier gas (N_2 density is 1.2506 kg/m^3), and thereby reduced degree of plastic deformation of the spray particles is expected for the coating. Thus, higher porosity levels, larger splat size, and reduced plastic deformation degree was observed when compared to those of helium-processed coating [19, 20]. Fig.5 (c) shows the surface morphology of the coating, revealing pores and voids and the presence of higher splats attributing to the multi-impacts on the coated layer. Figure 6 (a, b, c) show the as received powder cross-section, as-sprayed powder and microstructure of sprayed particle. It is interesting to note that the dendritic microstructure of the feedstock powder is also found on the as-sprayed sub layer of CGDS coating, consisting of interlocked dendrites, where most of the dendrites appear to be deformed significantly, giving a flattened appearance as compared to original dendrites of the feedstock powder. The EDAX analysis at some points was taken for confirmation of any change of chemical composition. The N_2 sprayed coating is almost same as the composition of the sprayed powder.

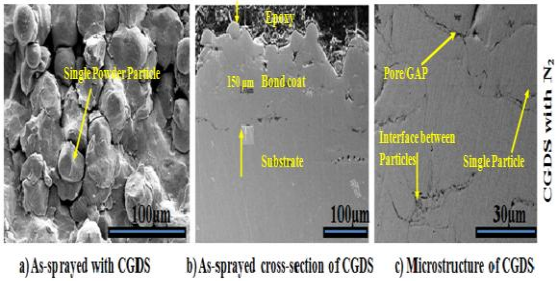

Fig. 5 SEM Image of CGDS Coating Sprayed With N_2 Gas in As-Sprayed Condition

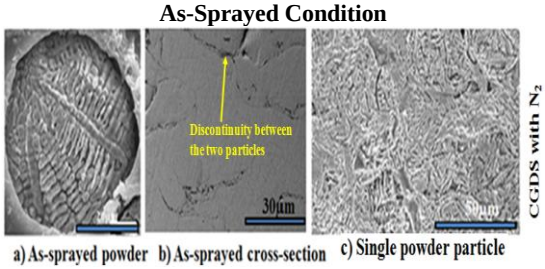

Fig. 6 (a) Secondary electron SEM images of etched cross section of powder revealing dendritic structure (b) As- sprayed CGDS cross-section revealing deformed dendrites (c) Single powder particle in deformed condition

Table 2 shows surface roughness and porosity measurement of CGDS sprayed with N_2 and HVOF coatings.

Table 2 Properties of HVOF and N_2-processed CoNiCrAlY sprayed deposition

Deposition properties	N_2 processing	HVOF processing
Microstructural features	Pores and porosity	Porosity and visible defect
Surfaces roughness Values Ra (µm)	16.04±1	8.41±0.55
Porosity level (%)	5±0.9	9±0.9

3.Nanoindentation analysis of the coatings

Fig.7 (a, b) show the nanoindentation measurements on coatings, CGDS sprayed with N_2 career gases and HVOF. A load of 11000, grams applied for 15 seconds and six indentations were made on each sample and the averages results were taken. The coating deposited by N_2 carrier gas was denser than that coated by HVOF. Table 3 shows values of hardness. The deposition hardness is dependent on the velocities attained by the particle, and thereby the impact to cause plastic deformation on the surface.

Table 3 Values of Nanoindentation

Process	Load P_{max} (mN)	Hardness (GPa)	Reduced modules Er (GPa)	Depth of penetration H_{max} (nm)
CGDS N_2	11000	6.35	151.33	250
HVOF	11000	5.04	119.10	285

Hence, the impact velocity, being a function of the ratio of specific heats and inversely to the mass of carrier gas, improves the hardness with lower density and higher specific heat ratio of carrier gas. Hence, pure nitrogen displayed higher hardness in contrast to HVOF processing conditions for deposition coatings [21].

ISSN: 2277-3754
ISO 9001:2008 Certified
International Journal of Engineering and Innovative Technology (IJEIT)
Volume 2, Issue 12, June 2013

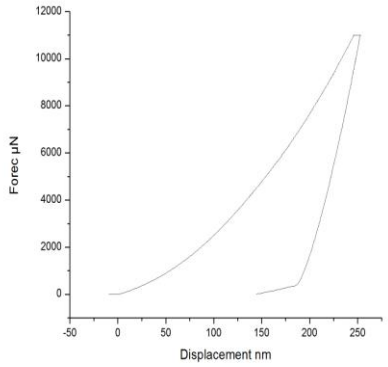

Fig. 7 (A) Nanoindentation Graphs Of CGDS Sprayed With N_2

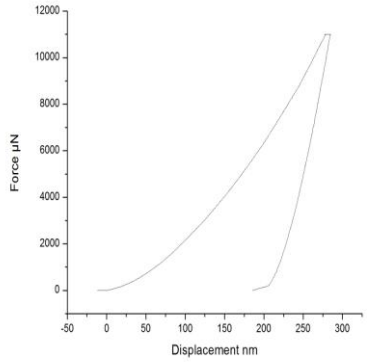

Fig. 7 (b) Nanoindentation graphs of HVOF

B. Oxidation Studies

1 Kinetics of HVOF and CGDS sprayed with N_2 coatings

The oxidation behavior of the coated stainless steel was investigated using discontinuous oxidation tests in air. The weight changes vs time plots for the oxidation of coatings in air at 900 ^{0}C are given in Fig.8. The linear plots appear to follow parabolic kinetics. The parabolic rate constants are determined using the equation. For evaluation, it is assumed that the oxidation follows a parabolic kinetic equation.

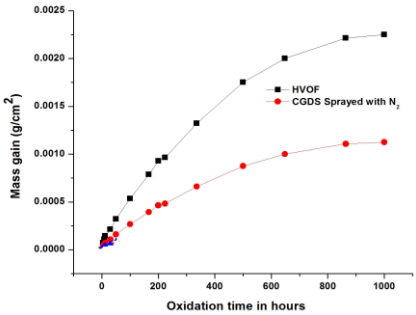

Fig. 8 Mass Gain Curve Obtained During Isothermal Oxidation of the HVOF and CGDS Sprayed With N_2 Coatings after the Oxidation at 900 ^{0}C for 1000 Hrs

$$\left(\frac{\Delta m}{A}\right)^2 = K_p t$$

Where Δm, mass gain in g; A, total surface area of the sample in cm^2; K_p, parabolic constant in g^2/cm^{4}s^{-1}; t, time in s. After 1000 hrs the parabolic rate constant, K_p calculated using parabolic equation was found to be 1.28x10^{-8} g^2/cm^{4}s^{-1}; for HVOF, 0.510x10^{-8} g^2/cm^{4}s^{-1}; for N_2 gas, sprayed with CGDS [17-19, 22]. The results show that the CGDS sprayed with N_2 coated samples shows significant lower oxidation rate than the HVOF coated samples.

2. Characterization of Oxidized scale of CGDS sprayed with N_2

Fig.9 shows the surface morphology of oxidized sample of CGDS sprayed with N_2 carrier gas coating oxidized at 900 ^{0}C for 200, 500 and 1000 hrs. The EDX analysis was done on oxidized surface was is rich in Al, and O and small amount of Cr and Co. It is clear from XRD (Fig.10) result that the intensity of the peaks associated to $CoCr_2O_4$ spinal-type oxides also increases, while the intensity of the α-Al_2O_3 peaks remains relatively low.

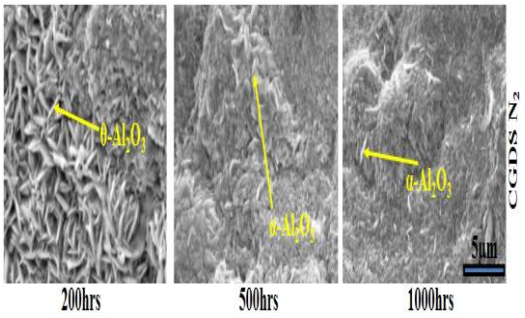

Fig. 9 Surface Morphology of the CGDS Coating Sprayed With N_2 Gas after the Oxidation at 900 ^{0}C for Different Times

XRD analysis carried out on the Feedstock powder was composed of γ and β-phases as depicted in Fig. 1. Fig.10 shows XRD results for the oxides formed at various stages of oxidation. It is observed that the as-sprayed coating do not retain the typical two-phase microstructure (γ-matrix Co-Ni-Cr solid solution and β-NiAl/CoAl precipitates) initially found in the feedstock powder [16, 17]. The absence of β-phase in as-sprayed coating shows that transformations of microstructure have taken place during deposition. In CGDS coating, the absence of the β-phase is in accordance with findings [16]. Fig. 11 shows cross-sectional morphology of oxidized samples. As oxidation time is increased up to 1000 hours for coating, it is clear from XRD (Fig.10) that the intensity of the peaks associated to $CoCr_2O_4$ spinal-type oxides and α-Al_2O_3 increases. N_2 coating contained many pores, which allowed oxygen to penetrate and form oxides within the coating. CGDS sprayed with N_2 porosity occurred in form of narrow but elongated gaps rather than as spheroidal structures. These gaps were located in between splats and thus impaired the adhesion of the splats. It was noticeable that the discontinuity between the two adjacent powder particles interface in the as-sprayed condition, led to preferred oxidation along the discontinuity boundaries due to the fast oxygen transportation along the discontinuities. After 1000 hrs of oxidation for and N_2 coatings however, the β-phase peaks are no longer discernable by XRD as the β-phase depletion zone has now reached a thickness that is greater than the penetration depth of the incoming x-rays.

ISSN: 2277-3754
ISO 9001:2008 Certified
International Journal of Engineering and Innovative Technology (IJEIT)
Volume 2, Issue 12, June 2013

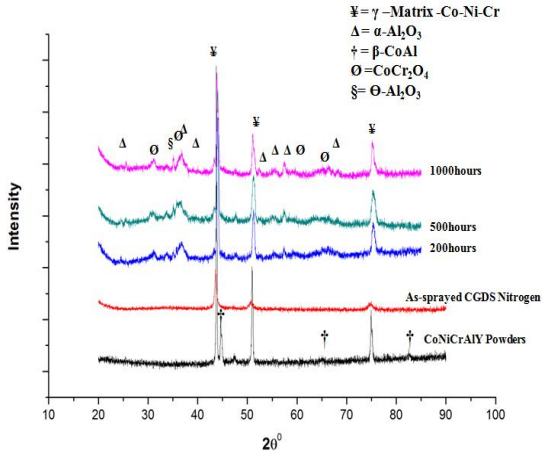

Fig. 10 XRD Patterns of Oxidized CGDS Coating Sprayed With N_2 Gas at the Temperature of 900 ^{0}C for Different Times

EDX spectra and composition of CGDS coating exposed at 900 ^{0}C for 1000 hrs reported in Fig. 12 showed that the sub scale TGO layer is rich in Al and O (Aluminum oxide), while the upper scale TGO layer contained other metallic oxides (Cr, and Co rich oxides).

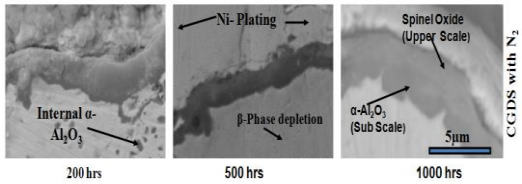

Fig. 11 Cross-Section Microstructure of the CGDS Coating Sprayed With N_2 Gas after the Oxidation at 900 ^{0}C for Different Times

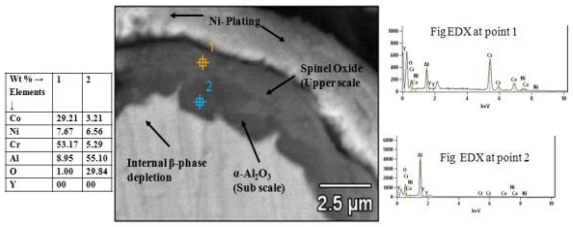

Fig. 12 the TGO bi-layered microstructure of the CGDS coating sprayed with N_2 gas after the oxidation at 900 ^{0}C for 1000 hrs

4 .Characterization of Oxidized scale of HVOF

Figure 13 illustrates surface morphology of HVOF coating oxidized at 900 ^{0}C for 200, 500 and 1000 hrs for isothermal oxidation. Surface scale morphology of the oxidized coating it can be seen that the surface is mostly covered with an oxides scale composed of aluminum and oxygen having needle-like (or whisker-like, blade like) morphology which is characteristics of α-Al_2O_3, and NiO and spinal-type oxides. The EDX analysis was done on oxidized surface was rich in Co, Ni and O rich oxide. Figure 14 shows XRD pattern of coating reveal the existence of NiO oxides, α-Al_2O_3 and the γ solid solution. As suggested by F. Tang, P. Richer, and Saeidi et al. [7, 17, 23], "spinel" represent wither a mixture of some/all of other spinel mixed oxides such as $NiCr_2O_4$, $NiAl_2O_4$, $CoAl_2O_4$, $CoCr_2O_4$ and $NiCo_2O_4$, or a substitutional solid solution of $(Ni, Co)(Al,Cr)_2O_4$.

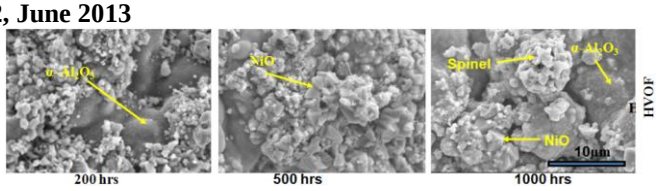

Fig.13 Oxide scale surface morphology of the HVOF coating after the oxidation at 900 ^{0}C for different times

From Fig. 13 for HVOF coating the surface morphology of the oxidized samples, it can be seen that the surface is the spinel-type oxides a mixture of a $(Ni,Co)(Al,Cr)_2O_4$, α-Al_2O_3 and also NiO.

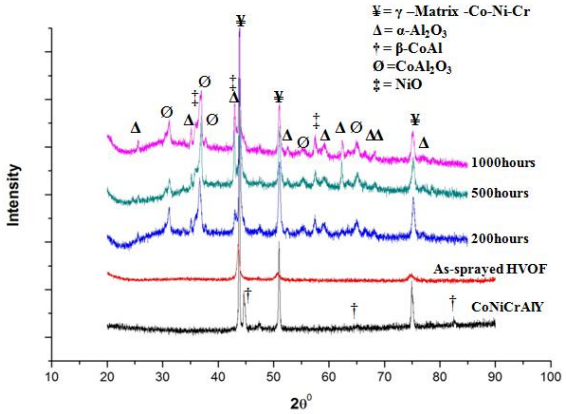

Fig. 14 XRD Patterns Of Oxidized HVOF Coating At The Temperature Of 900 ^{0}C For Different Times

Oxide layer formed at 1000 hrs reveals the presence of an area with higher Ni concentration, which corresponds to an oxide on the coating surface with block-shape morphology is typical NiO, the presence of this oxide suggests that the coating is nearing the end of its Al-rich lifecycle. These findings are in accordance with those reported in study [7, 23, and 24]. Figure 15 shows cross-sectional morphology of oxidized samples. As oxidation time is increased up to 1000 hours for coating, it is clear from XRD (Fig. 14) that the intensity of the peaks associated to α-Al_2O_3 and NiO increases. As oxidation of the coating progresses, aluminum diffuses from the β-precipitates and reacts to form α-Al_2O_3, NiO and spinal type of scale, thereby resulting in a β-phase depletion zone near the oxidized surface. HVOF coatings contained many pores, which allowed oxygen to penetrate and form oxides within the coating. After oxidation of 1000 hrs, the β-CoAl phase decreased with the increase of oxidation time.

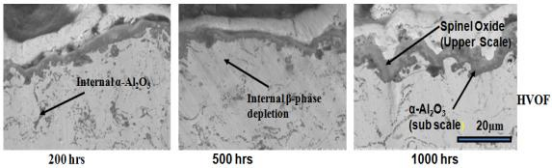

Fig. 15 Cross-section microstructure of the HVOF coating after the oxidation at 900 ^{0}C for different times

EDX spectra and composition of HVOF coating exposed at 900 ^{0}C for 1000 hrs reported in Fig. 16 showed that the sub scale TGO layer is rich in Al and O (Aluminum oxide), while the upper scale TGO layer contained other metallic oxides (Co, Ni and O rich oxide) [17, 22, 25]

ISSN: 2277-3754
ISO 9001:2008 Certified
International Journal of Engineering and Innovative Technology (IJEIT)
Volume 2, Issue 12, June 2013

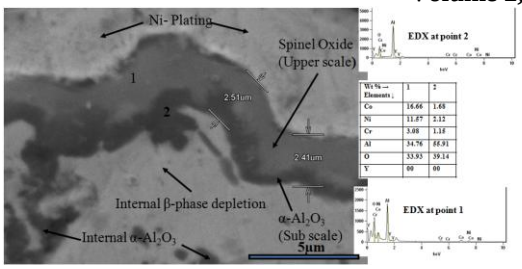

Fig. 16 the TGO Bi-Layered Microstructure of the HVOF Coatings at 900 ^{0}C for 1000 Hrs

IV. GENERAL DISCUSSIONS

In the present work, microstructural, morphological, and compositional analyses were conducted on sample coated by HVOF and CGDS techniques. A CoNiCrAlY powder of same composition was deposited onto 316L substrate. Samples were isothermally oxidized in furnace at 900 ^{0}C for different periods up to 1000 hrs. The coatings show different morphology and microstructure. It was observed that none of the as-sprayed coatings had retained the typical two-phase microstructure (γ-matrix Co–Ni–Cr solid solution and β-NiAl precipitates) initially found in the feedstock powder which was similar to the findings of P. Richer et al. [16, 17]. After isothermal oxidation tests, HVOF and CGDS coated with N_2 gas showed different morphological behavior and oxidation resistance. Overall oxide growth rates were minimal for the CGDS sprayed with N_2, followed closely by the HVOF coatings. HVOF coating shows the presence of sub layer of α-Al_2O_3 and upper layer of $(Ni,Co)(Al,Cr)_2O_4$ /$CoCr_2O_4$ spinal-type oxides$_3$ suggests that the coating is nearing the end of its Al-rich lifecycle. Duplex oxide scales similar to that in the present study have also been reported [7, 23, and 25].

V. CONCLUSION

- CoNiCrAlY powder was successfully deposited by the cold-spray technique using N_2 as accelerating gas.
- Cold-spray deposition of CoNiCrAlY powder using N_2 as carrier gas exhibited less dense morphological structure. This effect was attributed to the lower ratio of specific heats and high mass density of nitrogen as carrier gas.
- The oxide scale for the CGDS coating was predominantly composed of alumina, and initiation of growth of NiO or spinal-type mixed in thermally grown oxide layer.
- The oxide scale for the HVOF coating shows undesirable NiO and mixed spinal-type oxides during oxidation it suggests that the coating is nearing the end of its Al-rich lifecycle.

ACKNOWLEDGMENT

The authors wish to thank, ASB Industries, Ohio, USA, and Metallizing Equipment Pvt. Ltd. Jodhpur, India, for thermal spraying the bond coats samples.

REFERENCES

[1] P. K. Wright, A.G. Evans, "Mechanisms governing the performance of thermal barrier coating.'' Current Opinion in Solid State and Materials Science 4 (1999) pp.255-265.

[2] A.G. Evans, D.R. Mumm, J.W. Hutchinson, G.H. Meier, F.S. Petit, "Mechanisms controlling the durability of thermal barrier coatings.'' Prog. Materials Science 46 (2001) pp.505-553.

[3] K. Messaoudi, A.M. Huntz, B. Lesage, "Diffusion and growth mechanism of Al_2O_3 scales on ferritic Fe-Cr-Al alloys." Material. Sci. Eng. A 247 (1) (1998) pp. 248-262.

[4] M. Shibata, S. Kuroda, H. Murakami, M. Ode, M. Watanabe, Y. Sakamoto, "Comparison of microstructure and oxidation behavior of CoNiCrAlY bond coating prepared by different thermal spray process." Materials Transactions vol. 47, no.7 (2006) pp.1638-1642.

[5] W. Brandl, D. Toma, J. Kruger, H.J. Grabke, G. Matthaus, "The oxidation behavior of HVOF thermal sprayed MCrAlY coating.'' Surface Coating Technology vol.94–95(1–3) (1997) pp.21-26.

[6] D. Toma, W. Brandl, U. Koster, "Studies on the transient stage of oxidation of VPS and HVOF sprayed MCrAlY coating." Surface Coating Technology vol.120 (1999) pp.8-15.

[7] F. Tang, L. Ajdelsztajn, G.E. Kim, V. Provenzano, J.M. Schoenung, " Effects of surface oxidation during HVOF processing on the primary stage oxidation of a CoNiCrAlY coating." Surface Coating Technology. 185 (2004) pp.228-233.

[8] A.P. Alkhimov, A.N. Papyrin, V.F. Kosarev, N.I. Nesterovich, M.M. Shushpanov, US Patent 5 302 414, Gas-Dynamic Spraying Method for Applying a Coating, April 12, 1994.

[9] R.C. Dykhuizen, M.F. Smith, "Gas dynamic principles of cold spray.'' J. Therm. Spray Technol. 7 (2) (1998) pp.205-212.

[10] T. Stoltenhoff, H. Kreye, H.J. Richter, "An analysis of the cold spray process and its coating." J. Therm. Spray. Technol. 11 (4) (2002) pp. 542-550.

[11] L. Ajdelsztajn, B. Jodoin, G.E. Kim, J.M. Schoenung, "Cold spray deposition of nanocrystalline aluminum alloy." Metall. Mater. Trans. A 36 (2005) pp.657.

[12] C. Borchers, F. Gartner, T. Stoltenhoff, H. Kreye, "Microstructural and macroscopic properties of cold sprayed copper coating." J. Appl. Phys. vol.93 no.12 (2003) pp.10064-10070.

[13] T.H. Van Steenkiste, J.R. Smith, R.E. Teets, "Aluminum coating via kinetic spray with relatively large powder particle."Surf. Coat. Technol. 154 (2002) pp.237-252.

[14] C.J. Li, W.Y. Li, Y.Y. Wang, "Formation of metastable phases in cold sprayed soft metallic deposit." Surf. Coat. Technol. vol.198, (2005) pp.469-473.

[15] L. Ajdelsztajn, B. Jodoin, P. Richer, E. Sansoucy, E.J. Lavernia, "Cold gas dynamic spraying of iron-base amorphous alloy." J. Therm. Spray Technol. 15 (4) (2006) pp.495.

[16] P. Richer, A. Zuniga M. Yandouzi, B. Jodoin, "CoNiCrAlY microstructural changes induced during Cold Gas Dynamic Spraying." Surf. Coat. Technol. 203 (2008) pp.364-371.

[17] P. Richer, M. Yandouzi, L. Beauvais, and B. Jodoin, "Oxidation Behavior of CoNiCrAlY Bond Coats Produced by Plasma, HVOF and Cold Gas Dynamic Spraying." Surface and Coatings Technology, 204 (2010) pp. 3962-3974.

[18] Q. Zhang, C.J. Li, Y. Li, S. Zhang, X.R. Wang Q. Zhang, G.J. Yang, and C.X. Li, "Thermal Failure of Nanostructured

ISSN: 2277-3754
ISO 9001:2008 Certified
International Journal of Engineering and Innovative Technology (IJEIT)
Volume 2, Issue 12, June 2013

Thermal Barrier Coatings with Cold-Sprayed Nanostructured NiCrAlY Bond Coat", J. Therm. Spray Technol., 17(5-6), (2008) pp. 838-845.

[19] K. Balani, T. Laha, A. Agarwal, J. Karthikeyan, N. Munroe, "Effect of carrier gases on microstructural and electrochemical behavior of cold-sprayed 1100 aluminum coating", Surface & Coatings Technology 195 (2005) pp. 272– 279 .

[20] Alkimov A.P., Kosarev V.F. et.al., Sov. Phys. Dokl., 1990. 35(12), pp.1047-1049.

[21] Giovanni di Girolamo, Marco Alfano, Leonardo Pagnotta, Robert J.K.Wood, Jurgita Zekony, "Depth sensing nanoindentation of oxidized plasma sprayed CoNiCrAlY coating." Scientific research, 1 (2011) pp.51-53.

[22] F. Tang, L. Ajdelsztajn, J.M. Schoenung, Influence of Cryomilling on the Morphology and Composition of the Oxide Scales Formed on HVOF CoNiCrAlY Coatings Oxidation of metals vol.61 no.314, (2004) pp.219-238.

[23] S. Saeidi, K.T. Voisey, and D.G.Mc Cartney, "The Effect of Heat Treatment on the Oxidation Behavior of HVOF and VPS CoNiCrAlY Coatings." J. Therm. Spray Technol., 18(2), (2009) pp. 209-216.

[24] L.Ajdelsztain, J.A.Picas, G.E.Kim, F.L.Bastian, J.Schoenung, V. Provenzano, "Oxidation behavior of HVOF sprayed nanocrystalline NiCrAlY powder."Material Science and Engineering A 338 (1-2) (2002) pp.33-43.

[25] W.R. Chen, X. Wu, B.R. Marple, D.R. Nagy, P.C. Patnaik, "TGO growth behavior in TBC with APS and HVOF bond coats." Surf. Coat. Technol. 202 (2008) pp.2677-2683.

AUTHOR BIOGRAPHY

W. S. Rathod
B.E. (Metallurgy), M.E. (Production), Ph.D. (Registered in 2010 in Corrosion Science)
Publication:-6
Presented paper at US:- "Comparative Study of Oxidation Behavior of CoNiCrAlY Bond Coats Produced by Cold Gas Dynamic Spray and High Velocity Oxy-fuel process" was presented at North American Cold Spray Conference Bellevue, conference 2013, held at Washington USA, April 3rd-4th 2013,